

collision cross section and the number and spatial distributions of target neutrons whose hole excitation energies are sufficiently small to permit the residual nucleus to be stable against particle emission. We find that the same simple model seems adequate for the estimation of the cross sections for high-energy (p,n) reactions.

Considering the crudeness of the calculation, the values of E_k in Table IV are not to be taken too seriously. The important point is that despite the crudeness

of the calculation, the E_k , which are the only free parameters in the calculation, have both reasonable values and trends with changing mass number.

ACKNOWLEDGMENTS

We should like to thank Dr. Warren Goodell, Edmund Taylor, William Hunt, and their staffs and associates for the use of the facilities of the Nevis Laboratories.

Measurement of Pair-Production Cross Section near Threshold*

TOSHIMITSU YAMAZAKI† AND JACK M. HOLLANDER

Lawrence Radiation Laboratory, University of California, Berkeley, California

(Received 17 June 1965)

A determination has been made of the total pair production cross section near threshold in germanium ($Z=32$) with use of lithium-drifted germanium gamma-ray detectors. The experimental results show a systematic trend when compared with the theoretical cross sections of Bethe and Heitler. The ratio of the experimental cross section to the Bethe-Heitler theoretical value increases as the photon energy approaches threshold; however, the increase is more rapid than expected from the calculations of Jaeger and Hulme.

I. INTRODUCTION

PAIR production is one of the fundamental processes of the interaction of photons with matter. The theoretical treatment of this process was given by Bethe and Heitler¹ (hereafter referred to as BH) in 1934. They calculated the cross section on the basis of the Born approximation in which the interaction of the created electrons with the nucleus is considered to be a small perturbation. In this approximation, the total cross section is exactly proportional to Z^2 , and decreases very rapidly as the photon energy approaches the threshold $2mc^2$. The criterion for the validity of the Born approximation is that

$$Ze^2/\hbar v_+ \ll 1 \quad \text{and} \quad Ze^2/\hbar v_- \ll 1,$$

where v_+ and v_- are the velocities of the created positron and negatron, respectively, and Ze is the nuclear charge. These conditions are also expressed as

$$E_+ \text{ (and } E_-) \gg 1/[1 - (\alpha Z)^2]^{1/2},$$

where E_+ and E_- are total energies of the respective particles in units of mc^2 . In other words, the necessary condition for the validity of the BH formula is that the photon energy k in units of mc^2 be

$$k \gg 2/[1 - (\alpha Z)^2]^{1/2}.$$

* This work was done under the auspices of the U. S. Atomic Energy Commission.

† On leave from the Institute for Nuclear Study, University of Tokyo, Tokyo, Japan.

¹ H. A. Bethe and W. Heitler, Proc. Roy. Soc. (London) **A146**, 83 (1934).

This means that at energies near threshold, $2mc^2$, the BH formula may not be accurate.

Later, Jaeger and Hulme² and Jaeger³ (referred to hereafter as JH) calculated the cross section as well as the energy distribution without using the Born approximation. They obtained an asymmetric energy distribution between the positron and the negatron which is caused by the repulsion of the positron from and the attraction of the negatron to the nucleus. The total cross section for Pb was found to be considerably larger below 2.6 MeV than the BH value.

Most of the experimental determinations of the total pair-production cross section, σ_{pair} , have in the past been done by means of total photon absorption measurements.⁴ The total absorption coefficient, μ_{total} , consists of three parts, i.e., the photoelectric effect, the Compton effect, and pair production. Since the cross section for the Compton scattering, σ_{Compton} , is well known from the Klein-Nishina formula and the photoeffect is negligible in the relevant energy region, σ_{pair} can be deduced from μ_{total} . There have been many experimental studies made in this way. One of them, performed by Colgate,⁵ shows (1) good agreement of the experimental cross section for any material at 2.62, 4.47, and 6.13 MeV with the theoretical value given by BH and (2) a

² J. C. Jaeger and H. R. Hulme, Proc. Roy. Soc. (London) **A153**, 443 (1936).

³ J. C. Jaeger, Nature **137**, 781 (1936); **148**, 86 (1941).

⁴ See review articles, for instance: C. M. Davison and R. D. Evans, Rev. Mod. Phys. **24**, 79 (1952).

⁵ S. A. Colgate, Phys. Rev. **87**, 592 (1952).

TABLE I. Summary of results on σ_{pair} (relative) obtained from singles spectra.

Photon energy (MeV)	Isotope	$A_{\text{pair}}/A_{\text{photo}}$	η_{photo}	ϵ	Correction ^a factor	σ_{pair} (relative)
1.173	Co ⁶⁰	$4.0 \pm 1.0(-2)^b$	8.80	$3.5 \pm 0.9(-1)^b$	0.995	$3.5 \pm 0.9(-1)^b$
1.278	Na ²²	$1.1 \pm 0.2(-1)$	7.00	$7.7 \pm 1.4(-1)$	0.990	$7.8 \pm 1.4(-1)$
1.332	Co ⁶⁰	$1.93 \pm 0.10(-1)$	6.45	$1.25 \pm 0.06(0)$	0.987	$1.27 \pm 0.06(0)$
1.368	Na ²⁴	$2.50 \pm 0.20(-1)$	6.05	$1.51 \pm 0.12(0)$	0.985	$1.53 \pm 0.12(0)$
1.407	Eu ¹⁵²	$3.40 \pm 0.20(-1)$	5.60	$1.90 \pm 0.11(0)$	0.983	$1.93 \pm 0.11(0)$
1.477	Mo ^{93m}	$5.49 \pm 0.25(-1)$	5.15	$2.78 \pm 0.13(0)$	0.976	$2.85 \pm 0.13(0)$
1.596	La ¹⁴⁰	$9.40 \pm 0.50(-1)$	4.15	$3.90 \pm 0.21(0)$	0.967	$4.03 \pm 0.22(0)$
1.837	Y ⁸⁸	$2.43 \pm 0.10(0)$	3.03	$7.36 \pm 0.30(0)$	0.942	$7.81 \pm 0.32(0)$
2.185	Nb ⁹⁰	$5.89 \pm 0.20(0)$	2.05	$1.21 \pm 0.04(1)$	0.897	$1.35 \pm 0.05(1)$
2.318	Nb ⁹⁰	$7.42 \pm 0.20(0)$	1.73	$1.28 \pm 0.03(1)$	0.880	$1.45 \pm 0.04(1)$
2.754	Na ²⁴	$1.50 \pm 0.05(1)$	1.15	$1.73 \pm 0.06(1)$	0.840	$2.06 \pm 0.08(1)$

^a Calculated for the 5-mm-thick crystal.^b $4.0 \pm 1.0(-2) = (4.0 \pm 1.0) \times 10^{-2}$.

slow increase in cross section at high Z , as predicted by JH.^{2,3} However, there are no experimental absorption data below 2.6 MeV because the absorption method is inadequate for the low-energy region, where the contribution of pair production is very small compared with that of the Compton effect.

Hahn, Baldinger, and Huber,⁶ and later Dayton⁷ performed relative determinations of σ_{pair} at 2.6, 1.8, and 1.33 MeV by detecting annihilation events following pair production with two scintillation counters. These experiments show a deviation of σ_{pair} from the Z^2 dependence that is in close agreement with the calculations of JH. This direct method, however, cannot be used with radioactive sources that emit two or more gamma rays, because the equipment accepts all pair-production events without discriminating photon energies.

In this paper we report on a measurement of the pair-production cross sections near threshold, carried out with the use of lithium-drifted germanium gamma-ray detectors. The principle of the method is as follows: When a photon of energy kmc^2 ($k > 2$) creates an e^+e^- pair within a germanium crystal, the kinetic energy of the electron pair is nearly completely absorbed, whereas the annihilation photons almost always escape. Thus, most pair production events result in a "pair peak" at $(k-2)mc^2$, which is the so called "double-escape" peak. Since this peak is formed by a single process (whereas photopeaks and Compton background are due to multiple events), it is possible by measuring the intensities of the pair peaks as a function of incident photon energy to determine the shape of the pair-production cross-section curve.

The experimental procedure and results are described in the following section. Also described are the necessary corrections to the experimental data that permit the determination of the relative σ_{pair} curve. The experimental and theoretical cross sections are compared in Sec. III.

⁶ B. Hahn, E. Baldinger, and P. Huber, *Helv. Phys. Acta* **25**, 105 (1952).

⁷ I. Dayton, *Phys. Rev.* **89**, 544 (1953).

II. EXPERIMENTAL PROCEDURE AND RESULTS

A. Measurements With a Single Detector

Used in these measurements was a lithium-drifted germanium detector, 2 cm² × 5 mm thick, that has an energy resolution full width at half-maximum (FWHM) of 2.4 keV at 279 keV. The gamma-ray sources were placed at 4 cm from the surface of the detector. Some singles spectra obtained with this detector are shown in Fig. 1. Even when the incident photon energy is close to $2mc^2$, the pair peak can be readily identified by its energy, which can be rather accurately determined with the germanium detector system. The use of a lead absorber will provide further confirmation, if necessary, since it reduces the intensities of photopeaks of lower energy photons more effectively than it does the double-escape peaks from higher energy photons.

For each gamma-ray energy, A_{pair} and A_{photo} (areas of pair and photopeaks, respectively) were measured. The quantity

$$\epsilon \equiv \eta_{\text{photo}}(A_{\text{pair}}/A_{\text{photo}}),$$

where η_{photo} is the photo-peak efficiency of the crystal, gives the ratio of pair-peak yield to photon intensity for each incident photon energy. In order to get σ_{pair} some corrections are made to this value, which will be dis-

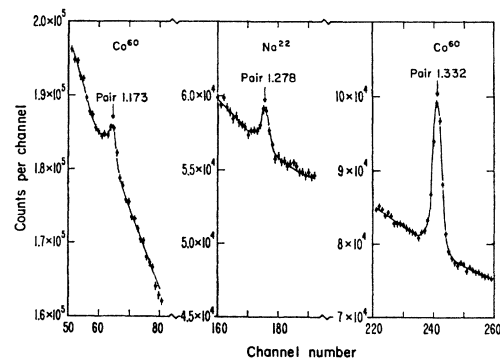


FIG. 1. Some singles spectra taken with a 2 cm² × 5 mm thick lithium-drifted germanium detector, showing the pair-production peaks from sources of Na²² and Co⁶⁰.

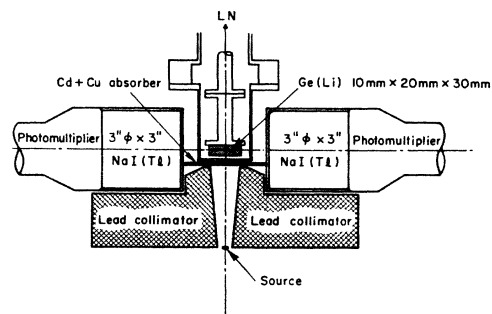


FIG. 2. Schematic view of the pair spectrometer.

cussed in Sec. II C. The experimental data obtained and resulting values of $\sigma_{\text{pair}}(\text{rel})$ are presented in Table I. At 1.17 MeV the ratio of peak to continuum is too small to allow an accurate value to be obtained.

B. Measurements with a Pair Spectrometer

A pair spectrometer was used in order to obtain pair-peak yields near threshold more accurately than could be done from the singles spectra. The apparatus, shown schematically in Fig. 2, consisted of a lithium-drifted germanium detector of size 20 mm \times 30 mm \times 10 mm and two 3 in. \times 3 in. NaI(Tl) scintillation counters. By adjusting the "windows" of both single-channel analyzers to accept the 511-keV photo-peak, the scintillation spectrometers thus detected annihilation-radiation pairs produced in the germanium crystal. A 400-channel pulse-height analyzer, gated by the annihilation events, displayed the pair spectrum. A block diagram of the conventional coincidence system is shown in Fig. 3. The resolving time of the triple coincidence circuit was varied from 40 to 60 nsec, according to the experimental situation. This system was carefully checked so as to achieve the same coincidence characteristics throughout the energy region studied.

The efficiency of the pair spectrometer, defined as the ratio of pair-peak counts in a pair spectrum to those in the corresponding singles spectrum, is independent of the incident photon energy, because it is simply expressed as $\Omega\eta^2$, where Ω and η are the geometrical efficiency and the photopeak efficiency of the NaI

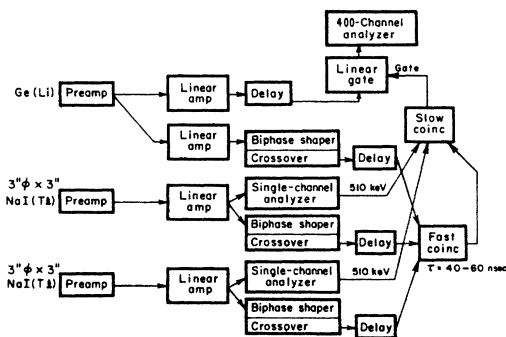


FIG. 3. Block circuit diagram of the pair spectrometer.

TABLE II. Relative pair-peak yields (ϵ), and σ_{pair} (relative) obtained with the pair spectrometer.

Photon energy (MeV)	Isotope	ϵ	Correction ^a factor	σ_{pair} (relative)
1.332	Co ⁶⁰	1.00	1.00	1.00
1.278	Na ²²	0.628 \pm 0.019	1.00	0.628 \pm 0.019
1.173	Co ⁶⁰	0.188 \pm 0.007	1.00	0.188 \pm 0.007
1.115	Zn ⁶⁵	0.054 \pm 0.004	1.00	0.054 \pm 0.004
1.077	Rb ⁸⁶	0.0138 \pm 0.0012	1.00	0.0138 \pm 0.0012

^a Calculated for the 10-mm thick crystal.

crystal for 511-keV photons, respectively. Actually, the efficiency was found to be 5%. By use of sources mixed with a standard source such as Co⁶⁰, it is possible to get good results even in the presence of small drifts in the system.

In the energy region of interest, near threshold, the pair-peak yield is so low that these peaks were not in fact visible in the singles spectrum of the germanium detector. Similarly, almost all the contributions to singles spectra of the scintillation spectrometers were due to gamma rays scattered from the germanium crystal and those that penetrated the lead collimator. Nevertheless, the coincidence pair spectra showed distinct peaks, as illustrated in Fig. 4, since the triple coincidence condition reduced considerably random coincidence rates.

The pair-peak intensities were obtained by integrating the peak areas above the continuous tail. Subtraction of the tail was believed to be the most effective means to remove the random coincidence counts. The relative pair-peak yields, ϵ , obtained in these experiments, are summarized in Table II. As will be seen later no correction is needed for these values, because the 10-mm thick crystal was used for low-energy photons, that is, ϵ is actually σ_{pair} (relative).

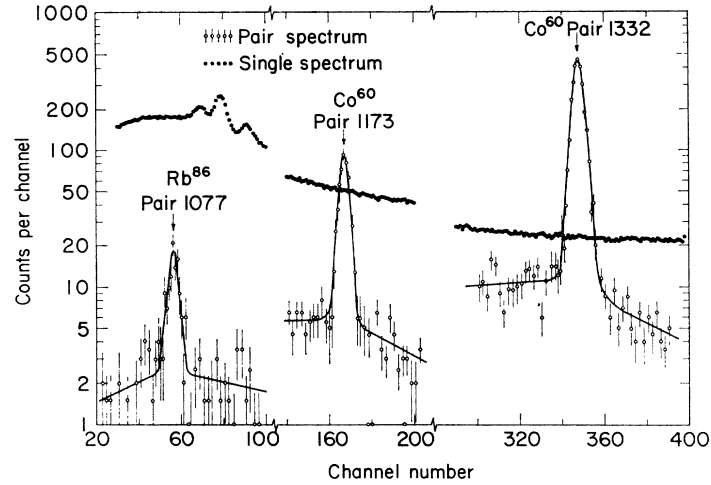
C. Corrections to Experimental Data

In order to deduce the total pair-production cross section, σ_{pair} , from the relative pair-peak yields ϵ the following corrections must be considered:

(1) Absorption of part or all of the annihilation photon energy in the crystal. This effect reduces the pair-peak yields; in the singles spectrum it shifts the pulse height of the pair peak to higher values (into the background) and in the coincidence spectrum it results in loss of 511-511 coincidences. However, because this effect always arises from the 511-keV photon, it has no energy dependence and hence is of no importance for relative measurements of σ_{pair} as a function of photon energy.

(2) Contribution of multiple processes resulting in pair peaks. At higher energy a scattered photon that has lost part of its energy in the crystal still contributes to pair production. The ratio α of this secondary

FIG. 4. Some pair spectra taken with the pair spectrometer, showing also singles spectra from the same sources.



process to the single process is given roughly by

$$\alpha \approx \left(\frac{1}{2}d\right) \mu_{\text{Compton}} \frac{\int_2^k \sigma_{\text{pair}}(k_1) dk_1}{(k - k_{\text{min}}) \sigma_{\text{pair}}(k)},$$

where d is the thickness of the crystal, μ_{Compton} is the Compton absorption coefficient at energy kmc^2 , and $k_{\text{min}}mc^2$ is the minimum energy of scattered photons. In Fig. 5 values of α are presented as a function of incident energy. This figure shows that this correction is quite negligible in the present case where the thickness of the crystal was 5 and 10 mm.

(3) Reduction of the incident photon flux in a crystal of finite thickness. Because the total absorption coefficient of gamma rays μ depends on the energy, the attenuation factor $e^{-\mu z}$ is energy-dependent. This correction is more important when the crystal is thicker.

(4) Incomplete absorption of positron-negatron pairs in the finite crystal. The probability of complete ab-

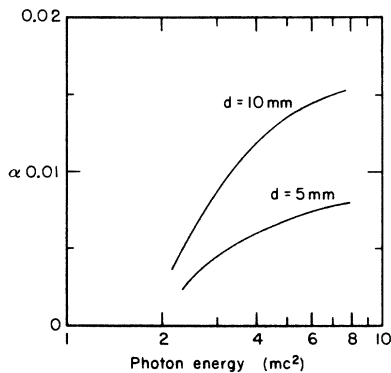


FIG. 5. Rough estimate of a ratio α of multiple processes to single process in formation of a pair peak.

sorption decreases as the incident energy increases. This effect, arising in the crystal surface, is considerable unless the crystal is sufficiently thick.

These two corrections were combined, and a numerical calculation was performed. A detailed description is presented in the Appendix. The obtained correction factors are illustrated in Fig. 6. The correction is at most 20% for a 5-mm thick crystal, and 6% for a 10-mm thick crystal at 2.75 MeV.

In order to confirm these correction factors experimentally, a pair spectrum of Na^{24} was measured with the 10-mm thick crystal as shown in Fig. 7. It seems that the lower-side plateau of 2.754-MeV pair peak, which is about 22% of the total, might be due to the incomplete absorption of positron-negatron pairs. However, there is a similar plateau at the 1.368-MeV pair peak, which is about 15% of the total. The difference is only 7%, which is consistent with the calculated value of 6%. Therefore, the main source of these plateaus must be attributed to another origin.

The correction factors for the 5-mm thick crystal are presented in column 6 of Table I. The relative values of σ_{pair} are tabulated in column 7. As for Table II no correction is necessary, because the energies were sufficiently low and the 10-mm thick crystal was used.

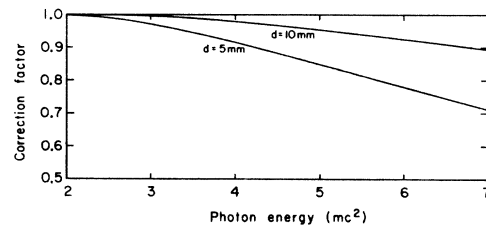


FIG. 6. Over-all correction factor to pair-peak yields as a function of incident photon energy, for detector thicknesses of 5 and 10 mm.

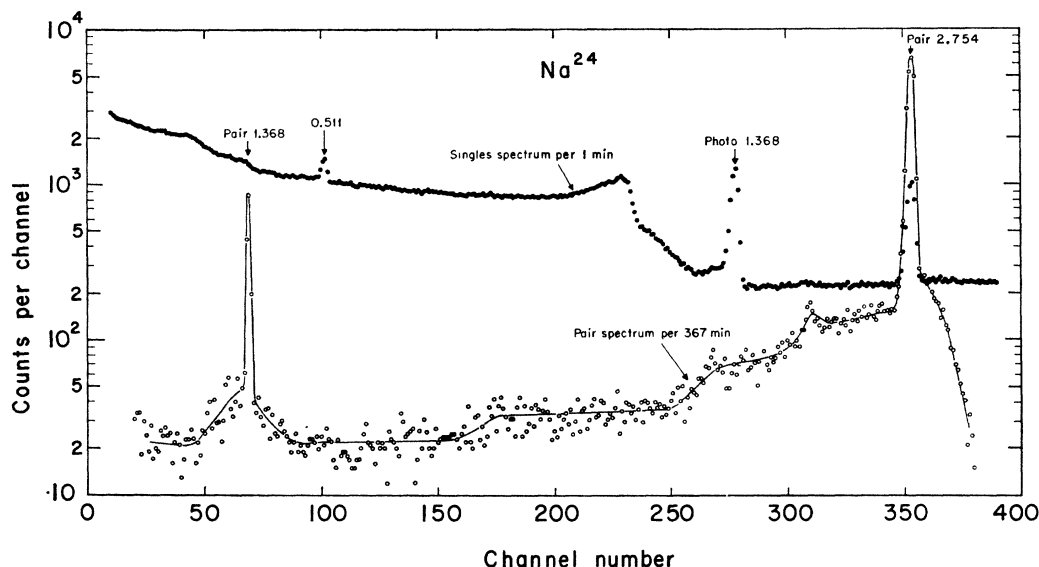


FIG. 7. Singles and pair-spectrometer spectra from Na^{24} . Dimensions of the Ge(Li) detector were: 20 mm \times 30 mm \times 10 mm.

III. PAIR-PRODUCTION CROSS SECTION

A. Theoretical Predictions

The differential cross section given by Bethe and Heitler¹ is as follows:

$$\begin{aligned} \Phi(E_+)dE_+ = & \bar{\phi} \frac{p_+ p_-}{k^3} dE_+ \left\{ -\frac{4}{3} - 2E_+ E_- \frac{p_+^2 + p_-^2}{p_+^2 p_-^2} \right. \\ & + \frac{E_+ \epsilon_-}{p_+^3} + \frac{E_- \epsilon_+}{p_+^3} - \frac{\epsilon_+ \epsilon_-}{p_+ p_-} \\ & + L \left[\frac{k^2}{p_+^3 p_-^3} (E_+^2 E_-^2 + p_+^2 p_-^2) - \frac{8 E_+ E_-}{3 p_+ p_-} - \frac{k}{2 p_+ p_-} \right. \\ & \left. \left. \times \left(\frac{E_+ E_- - p_-^2}{p_-^3} \epsilon_- + \frac{E_+ E_- - p_+^2}{p_+^3} \epsilon_+ + \frac{2k E_+ E_-}{p_+^2 p_-^2} \right) \right] \right\}, \end{aligned} \quad (1)$$

where E_+ and E_- are the total energies of positron and negatron in units of mc^2 , respectively, and p_+ and p_- are the momenta of the respective particles, and the other quantities are defined by

$$\epsilon_+ = 2 \ln(E_+ + p_+), \quad \epsilon_- = 2 \ln(E_- + p_-),$$

$$L = 2 \ln[(E_+ E_- + p_+ p_- + 1)/k],$$

and

$$\bar{\phi} = Z^2 r_0^2 / 137.$$

We have calculated the total cross section σ_{pair} by numerical integration of $\Phi(E_+)$, that is,

$$\sigma_{\text{pair}}(\text{BH}) = \int_1^{k-1} \Phi(E_+) dE_+.$$

The results are tabulated in Table III. In Fig. 8 the energy dependence of σ_{pair} (BH) is shown.

Jaeger and Hulme² and later Jaeger³ made more realistic calculations of σ_{pair} involving the interaction between nucleus and electrons. They obtained numerical values of σ_{pair} for $Z=50, 65,$ and 82 at $k=3.0$ and 5.2 .

TABLE III. Total pair-production cross sections in units of $\bar{\phi} = Z^2 r_0^2 / 137$ calculated with the Bethe-Heitler formula.

k	$\sigma_{\text{pair}}/\bar{\phi}$	k	$\sigma_{\text{pair}}/\bar{\phi}$
2.020	0.2027(-5)*	3.700	0.2462(0)
2.030	0.6779(-5)	3.800	0.2725(0)
2.040	0.1586(-4)	3.900	0.2993(0)
2.050	0.3058(-4)	4.000	0.3266(0)
2.060	0.5213(-4)	4.200	0.3826(0)
2.070	0.8170(-4)	4.400	0.4398(0)
2.080	0.1204(-3)	4.600	0.4979(0)
2.100	0.2290(-3)	4.800	0.5565(0)
2.120	0.3856(-3)	5.000	0.6155(0)
2.140	0.5967(-3)	5.200	0.6747(0)
2.160	0.8684(-3)	5.400	0.7337(0)
2.180	0.1206(-2)	5.600	0.7926(0)
2.200	0.1613(-2)	5.800	0.8512(0)
2.250	0.2964(-2)	6.000	0.9095(0)
2.300	0.4825(-2)	6.500	0.1053(1)
2.350	0.7227(-2)	7.000	0.1193(1)
2.400	0.1019(-1)	7.500	0.1329(1)
2.450	0.1372(-1)	8.000	0.1461(1)
2.500	0.1782(-1)	8.500	0.1589(1)
2.600	0.2769(-1)	9.000	0.1713(1)
2.700	0.3974(-1)	9.500	0.1834(1)
2.800	0.5380(-1)	10.000	0.1950(1)
2.900	0.6973(-1)	11.000	0.2172(1)
3.000	0.8738(-1)	12.000	0.2382(1)
3.100	0.1066(0)	13.000	0.2579(1)
3.200	0.1271(0)	15.000	0.2942(1)
3.300	0.1490(0)	20.000	0.3708(1)
3.400	0.1719(0)	30.000	0.4846(1)
3.500	0.1959(0)	50.000	0.6346(1)
3.600	0.2207(0)		

* 0.2027(-5) = 0.2027 $\times 10^{-5}$.

In order to deduce σ_{pair} for $Z=32$ the following empirical formula suggested by JH may be used:

$$\sigma_{\text{pair}}(\text{JH})/\sigma_{\text{pair}}(\text{BH}) = 1 + a(k)Z^2, \quad (2)$$

where $a(k)$ is a parameter depending only on the photon energy. This ratio for Ge was found to be 1.15 and 1.04 at $k=3.0$ and 5.2, respectively, with use of the JH calculated values for $Z=50, 65,$ and 82. Here pair production in the electron field (triplet production) is neglected, because the cross section is about 1% of that in the nuclear field and the threshold energy is $4mc^2$.⁸

B. Experimental Values

As mentioned in Sec. I, previous experiments have shown good agreement with the BH prediction at 2.6 MeV. The present experimental data have been normalized, as shown in Table IV, so as to agree with the JH calculation at 2.754 MeV, which is only 4% higher than the BH value. The experimental values are plotted in Fig. 8 together with the BH curve.

In column 5 of Table IV $\sigma_{\text{pair}}(\text{BH})$ is given, and the ratio of $\sigma_{\text{pair}}(\text{exptl})$ to $\sigma_{\text{pair}}(\text{BH})$ in column 6. These ratios, giving deviations from the BH prediction, are plotted as a function of energy above threshold in Fig. 9. This figure also includes the theoretical curve predicted by JH and experimental points (shown as triangles) which are interpolated from the experiments of Hahn *et al.*⁶ and of Dayton⁷ using the empirical formula (2). It is clearly seen that the ratio increases as the photon energy approaches the threshold. This systematic trend agrees qualitatively with the theory of Jaeger and Hulme, but the deviation seems more striking than expected from their calculation.

TABLE IV. Experimental pair-production cross sections in comparison with the Bethe-Heitler cross sections.

Photon energy (MeV)	k	Isotope	$\sigma_{\text{pair}}(\text{exptl})$	$\sigma_{\text{pair}}(\text{BH})$	$\sigma_{\text{pair}}(\text{exptl})/\sigma_{\text{pair}}(\text{BH})$
1.077	2.108	Rb ⁸⁶	$5.76 \pm 0.50 (-4)^a$	$2.855 (-4)^a$	2.02 ± 0.18
1.115	2.182	Zn ⁶⁵	$2.33 \pm 0.17 (-3)$	$1.243 (-3)$	1.82 ± 0.14
1.173	2.295	Co ⁶⁰	$7.86 \pm 0.29 (-3)$	$4.614 (-3)$	1.70 ± 0.07
1.278	2.500	Na ²²	$2.63 \pm 0.08 (-2)$	$1.781 (-2)$	1.48 ± 0.05
1.332	2.607	Co ⁶⁰	$4.18 \pm 0.13 (-2)$	$2.846 (-2)$	1.47 ± 0.05
1.368	2.677	Na ²⁴	$5.18 \pm 0.16 (-2)^b$	$3.677 (-2)$	1.41 ± 0.04
1.407	2.753	Eu ¹⁵²	$6.36 \pm 0.36 (-2)$	$4.693 (-2)$	1.36 ± 0.08
1.477	2.890	Mo ^{93m}	$9.39 \pm 0.43 (-2)$	$6.804 (-2)$	1.38 ± 0.07
1.596	3.123	La ¹⁴⁰	$1.32 \pm 0.07 (-1)$	$1.112 (-1)$	1.19 ± 0.06
1.837	3.594	Y ⁸⁸	$2.58 \pm 0.11 (-1)$	$2.191 (-1)$	1.18 ± 0.05
2.185	4.276	Nb ⁹⁰	$4.43 \pm 0.16 (-1)$	$4.041 (-1)$	1.10 ± 0.04
2.318	4.536	Nb ⁹⁰	$4.78 \pm 0.13 (-1)$	$4.791 (-1)$	1.00 ± 0.03
2.754	5.389	Na ²⁴	$7.60 \pm 0.23 (-1)^{b,c}$	$7.303 (-1)$	1.04 ± 0.03

^a $5.76 \pm 0.50 (-4) = (5.76 \pm 0.50) \times 10^{-4}$

^b These relative values were obtained from a pair spectrum of Na²⁴, being considered as most reliable.

^c Normalized at 2.754 MeV to the JH value, which is 4% higher than the BH value.

⁸ See review articles, H. A. Bethe and J. Ashkin, in *Experimental Nuclear Physics, Vol. I*, edited by E. Segrè (John Wiley & Sons, Inc., New York, 1953), p. 2; D. R. Corson and A. O. Hanson, *Ann. Rev. Nucl. Sci.* 3, 67 (1953); C. M. Davisson, in *Alpha-, Beta- and Gamma-Ray Spectroscopy*, edited by K. Siegbahn (North-Holland Publishing Company, Amsterdam, 1965), p. 37.

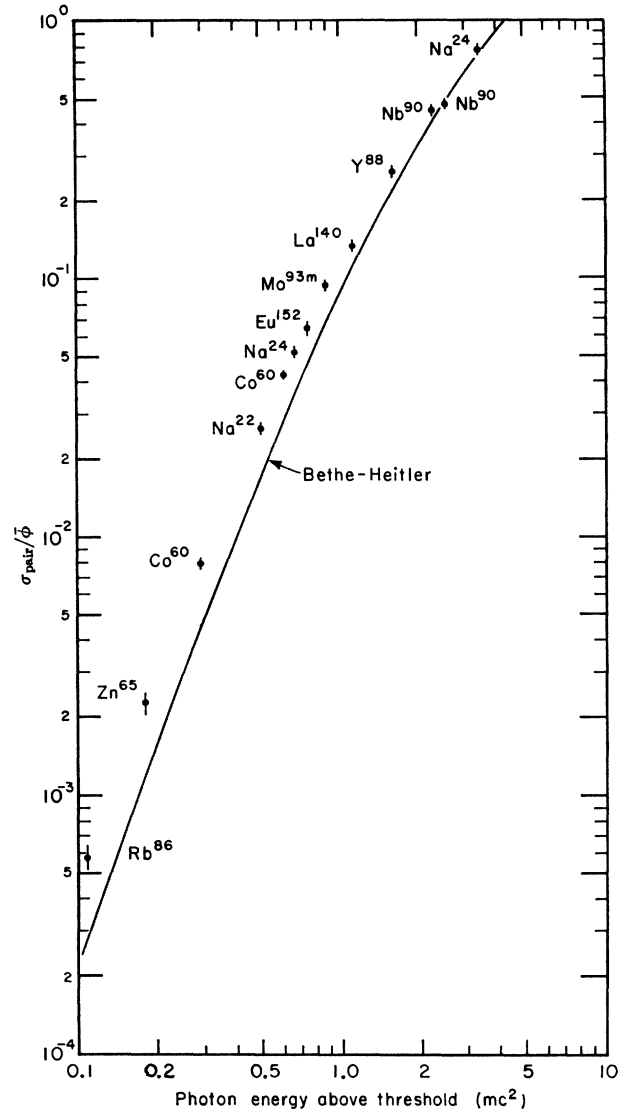


FIG. 8. Pair-production cross section versus photon energy above threshold. The calculated Bethe-Heitler curve is shown together with the experimental values, normalized at 2.754 MeV as described in the text.

IV. CONCLUSION

In the work reported here, semiconductor detectors have been applied to the investigation of an elementary process, pair-production. With the method described, pair-production cross sections have been measured for photon energies as low as 1.077 MeV. With improvements in the technique, it should be possible to lower the experimental limit more closely to the threshold. It appears, from the estimates of experimental corrections to the data, that the thickness of germanium crystals used in the present experiment is near to optimum for this type of measurement. If a very large crystal were to be used, multiple processes in formation of pair peaks would become considerable, and if a very

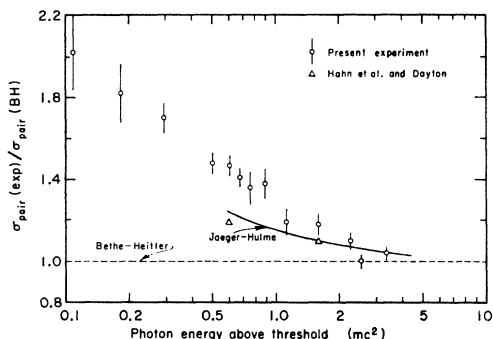


FIG. 9. The ratio of $\sigma_{\text{pair}}(\text{exptl})/\sigma_{\text{pair}}(\text{BH})$. The JH curve extrapolated from high- Z values is also shown. The triangles represent interpolated values from the experiments of Hahn *et al.* (Ref. 6) and of Dayton (Ref. 7).

thin one were used, a large fraction of the pair production events would be lost from the pair peaks because of the surface effect. In both cases the reliability of the cross sections derived from the experimental data would be reduced.

The experimental results have revealed a systematic behavior of the cross section near the threshold. As the photon energy decreases, the ratio of the experimental cross section to the Bethe-Heitler cross section based on the Born approximation gradually increases. This ratio reaches a value of about 2 at 1.077 MeV. This feature is in qualitative agreement with the calculation of Jaeger and Hulme, which takes into account the interaction between nucleus and produced electrons. Although there is no quantitative theoretical calculation in the relevant energy region, the systematic deviation seems more conspicuous than expected from the prediction of Jaeger and Hulme.

ACKNOWLEDGMENTS

We wish to express our appreciation for the assistance of C. J. Butler in setting up the pair spectrometer, of R. A. Gembala in assembling and testing the electronics system, and of J. A. Harris in the preparation of sources. One of the authors (T. Y.) wishes to express his gratitude to the Miller Institute of the University of California for the receipt of a Miller Research Fellowship and to Professor I. Perlman and Professor J. O. Rasmussen for their hospitality and encouragement.

APPENDIX: CORRECTION FOR INCOMPLETE ABSORPTION OF PAIRS NEAR THE SURFACE OF A GERMANIUM CRYSTAL

In order to deduce the pair-production cross section from the pair-peak yield, a correction should be made for the incomplete absorption of negatron-positron pairs produced near the surface of the crystal. Since this correction is significant at higher energy and in this case created pairs are emitted mostly forward, consideration of a simplified one-dimensional problem will be sufficient.

The direction of incident photons is assumed to be normal to the surface of a crystal of thickness d millimeters. An event of pair production is illustrated in Fig. 10. In general, the created electrons have a complicated angular distribution. However, the following simple approximate formula is well known⁸:

$$\Phi(\theta)d\theta = \frac{\theta d\theta}{\Theta^2 + \theta^2}, \quad \Theta = \frac{1}{E},$$

where Φ is the number of electrons of total energy E in units of mc^2 emitted at an angle θ . For the present purpose it is assumed that negatrons and positrons are emitted at fixed angles θ_- and θ_+ , respectively, which are set at the most probable angles.

$$\theta_- = \frac{1}{\sqrt{3}E_-}, \quad \text{and} \quad \theta_+ = \frac{1}{\sqrt{3}E_+}.$$

Moreover, it is assumed that the negatrons and positrons do not change direction until they have passed their practical ranges, R_+ and R_- and have lost their kinetic energies. The practical range R in mm of an electron of kinetic energy T in mc^2 is approximated by the formula⁹

$$R = 0.503T - 0.176[1 - \exp(-T/0.36)].$$

The available lengths L_- and L_+ in the germanium crystal (see Fig. 10) are simply

$$L_- = (d-z)/\cos\theta_- \quad \text{and} \quad L_+ = (d-z)/\cos\theta_+.$$

The probability that a measured electron pair is created at depth z with positron energy E_+ is given by a step function

$$F(E_+, z) = 1, \quad \text{when } L_- > R_- \text{ and } L_+ > R_+ \\ = 0, \quad \text{otherwise.}$$

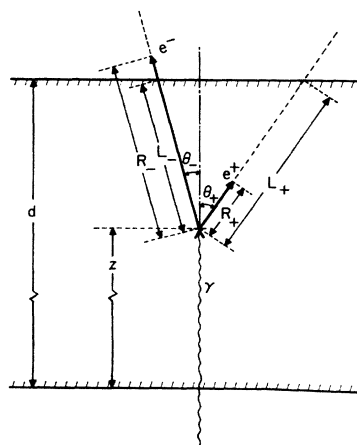


FIG. 10. Diagram of a pair-production event in a germanium crystal.

⁹ G. Knop and W. Paul, in *Alpha-, Beta- and Gamma-Ray Spectroscopy*, edited by K. Siegbahn (North-Holland Publishing Company, Amsterdam, 1965), p. 1.

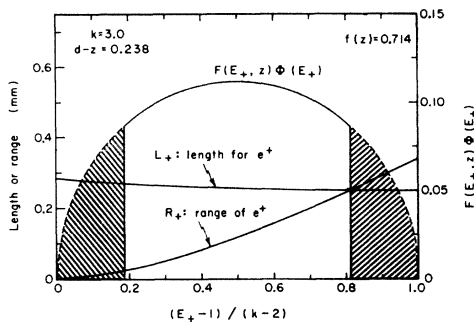


FIG. 11. Illustration of length L , range R , and the probability function versus positron energy.

Then $f(z)$, the efficiency for detecting pairs produced by a photon of energy k , is expressed as

$$f(z) = \int_1^{k-1} F(E_+, z) \Phi(E_+) dE_+ / \int_1^{k-1} \Phi(E_+) dE_+,$$

where $\Phi(E_+)$, the differential cross section of pair production, is given in Eq. (1). Of course, all these values depend on the incident photon energy. An example of the variation of L_+ , R_+ , and $F(E_+, z)$ and $\Phi(E_+)$ with E_+ is presented in Fig. 11. The shaded area corresponds to the number of pairs that do not contribute to the

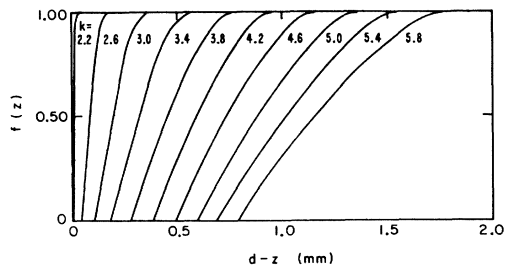


FIG. 12. The pair-detection efficiency factor $f(z)$ versus $d-z$ for an incident energy.

formation of a pair peak because of the incomplete absorption of total kinetic energy. The function $f(z)$ is illustrated in Fig. 12 with various photon energies.

The over-all correction factor g was obtained by integration of $f(z)$:

$$g = \frac{1}{d} \int_0^d f(z) e^{-\mu z} dz,$$

where μ is the total absorption coefficient of photons. The dependence of g on photon energy is presented in Fig. 6 after normalization at $k=2.0$.

The numerical calculation was performed with the use of an IBM 7094 computer.